# Global Prediction of Thermal Soil Regimes

J.M.H. Hendrickx[1*], H. Xie[2], J.B.J. Harrison[1],
B. Borchers[1] and J. Simunek[3]

[1] New Mexico Tech, Socorro, NM
[2] University of Texas, San Antonio, TX
[3] University of California, Riverside, CA

## ABSTRACT

A thorough understanding of thermal soil regimes is critical information for a wide variety of disciplines and engineering applications as well as for the evaluation of potential and limitations of thermal and optical sensors. In this study we have developed a procedure for the evaluation of global thermal soil regimes. First, pedotransfer functions are used to derive thermal soil properties (volumetric soil heat capacity and thermal conductivity) from readily available soil data on texture, bulk density, and organic carbon. Next, the average annual soil temperature is derived from the average annual air temperature. Then, the thermal top boundaries are derived either for well-watered sites using the daily and annual air temperature amplitudes as proxies for the daily and annual soil surface temperature amplitudes or for a wide range of environmental conditions using the model HYDRUS1D. A thorough validation of the proposed procedure is needed for the quantification of the probability with which soil thermal regimes can be predicted.

**Keywords:** soil thermal properties, soil thermal regimes, soil temperature

## 1. INTRODUCTION

A thorough understanding of thermal soil regimes is critical information for a wide variety of disciplines and engineering applications. The earliest studies of soil temperature started in agriculture since the germination of seeds early in the growing season depends to a large extent on soil temperature. Other agricultural processes depending on soil temperature are bacterial growth and plant production, decomposition and mineralization of organic matter, and microbiological rate processes such as the biodegradation of organic chemicals [1-3].

One expression of soil thermal regimes is the soil surface temperature that influences thermal and optical sensors. The detection probability of targets by thermal sensors is greatly influenced by the spatial-temporal distributions of thermal backgrounds such as soils [4, 5]. Thermal signatures of IED's and tunnels are determined by the thermal regime of the surrounding soil. The research group of the senior author has investigated extensively the complex interactions between landmines, soil conditions, and the temporal behaviors of thermal signatures of landmines and Improvised Explosive Devices (IED's) [6-9].

Optical sensors are strongly affected by the structure parameter of the air $C_n^2$ that is directly influenced by soil surface temperature. Knowledge of soil thermal properties and regimes is necessary information for the prediction of the temporal dynamics of the spatial distributions of $C_n^2$ profiles in the atmospheric boundary layer. Relationships between soil surface temperatures, sensible heat fluxes, and $C_n^2$ have been measured and evaluated using scintillometers and remote sensing by the research group of the senior author [10-12]. This study is an important part of these other ongoing investigations that aim at estimating all components of the energy balance under clear, partly cloudy, and overcast conditions using satellite imagery. Its main objective is to develop a procedure for the estimation of global distributions of soil thermal properties and global thermal boundary conditions that then can be used for the prediction of global thermal soil regimes.

---
[*] Jan_Hendrickx_NMT@msn.com; phone: 575-835-5892; 801 LeRoy Place, NMT/MSEC 240, Socorro NM 87801.

## 2. PHYSICS OF SOIL HEAT FLOW

The heat flow equation is

$$\frac{\partial T}{\partial t} = \frac{\lambda}{C} \frac{\partial^2 T}{\partial z^2} = \alpha \frac{\partial^2 T}{\partial z^2}$$

[1]

where $T$ is temperature (°C), $t$ is time (s), $\lambda$ is thermal conductivity (W m$^{-1}$ °C$^{-1}$), $C$ is volumetric heat capacity (J m$^{-3}$ °C$^{-1}$), $\alpha$ is thermal diffusivity (m$^2$ s$^{-1}$), and $z$ is depth (m) [2]. To solve this equation information is needed about the thermal soil properties (*thermal conductivity* and *volumetric heat capacity* or the *thermal diffusivity*) and the *thermal top and bottom boundary conditions* of the soil profile under consideration.

Since the solar heat source at the soil surface is periodic with daily and annual cycles, it can be assumed that the soil temperature at great depth will be approximately constant and will stay equal to the annual average temperature ($T_{avg}$). Therefore, the *thermal bottom boundary condition* is

$$\lim_{z \to -\infty} T(z,t) = T_{avg}$$

[2]

The depth where temperature remains constant is not the same for all soils since it depends on climate and latitude. Seasonal fluctuations of soil temperature have been estimated to penetrate to a depth of 20 m in Alaska, 15 m in midlatitudes, and 10 m in the Tropics [13].

The *thermal top boundary condition* of a soil profile is a complex function of incoming and reflected solar radiation, outgoing and incoming longwave radiation, topography, soil moisture, weather conditions, and vegetative cover [2, 3]. Therefore, daily soil temperature regimes close to the soil surface are best evaluated using numerical models such as HYDRUS1D ([14]. Nevertheless, a good understanding of thermal soil regimes can be obtained by approximating the soil surface temperature as a harmonic function that fluctuates with a daily and/or annual cycle.

$$T(t) = T_{avg} + A \sin(\omega t + \varphi)$$

[3]

where $A$ is the amplitude of the surface temperature fluctuation, $\varphi$ is a phase constant, and $\omega = 2\pi/\tau$ is the angular frequency where $\tau$ is the period of the wave.

The solution of heat flow Eq. [1] for a uniform soil exposed to a soil surface temperature that harmonically fluctuates with a daily and annual cycle is presented by Van Wijk (1963)

$$T(z,t) = T_{avg}^{annual} + A_0^{annual} e^{-\frac{z}{D_{annual}}} \sin(\omega_{annual} t + \varphi_0^{annual} - \frac{z}{D_{annual}})$$

[4]

$$+ A_0^{daily} e^{-\frac{z}{D_{daily}}} \sin(\omega_{daily} t + \varphi_0^{daily} - \frac{z}{D_{daily}})$$

where $T_{avg}^{annual}$ is the mean average annual soil profile temperature, $A_0^{annual}$ is the amplitude of the annual soil surface temperature variation, $A_0^{daily}$ is the amplitude of the daily soil surface temperature variation, $D_{annual}$ is the annual damping depth (m), $D_{daily}$ is the daily damping depth (m), $\omega_{annual}$ is the annual radial frequency, $\omega_{daily}$ is the daily radial frequency, $\varphi_{annual}$ is the annual phase constant, and $\varphi_{daily}$ is the daily phase constant. In Eq. [4] the amplitude of the daily soil surface temperature variation is assumed constant which generally is not the case. Therefore, a solution for Eq. [1] has been developed that allows for a temporal variation of the daily soil surface temperature amplitude during the year[15].

The damping depth $D$ is

$$D = \sqrt{\frac{2\lambda}{C\omega}} = \sqrt{\frac{2\alpha}{\omega}}$$

[5]

and the phase constant $\varphi$ is

$$\varphi = -\omega\, t_0$$

[6]

where $t_o$ is an arbitrary zero point in time. Thus, for the evaluation of global thermal soil regimes the required information is (1) the global distribution of thermal soil properties (thermal conductivity and volumetric heat capacity) and (2) the global distribution of the thermal top and boundary conditions (the annual average soil temperature, the amplitudes of the annual and daily soil surface temperature).

## 3. GLOBAL DISTRIBUTION OF SOIL THERMAL PROPERTIES

### 3.1. From Qualitative to Quantitative Soil Information

No map exists with the worldwide distribution of soil thermal properties. In fact, the only worldwide map with soil information is the FAO-Unesco Soil Map of the World. This map is a compilation of approximately 600 soil maps of different scales and legends. The map was first published in 1974 and digitized in 1995[16]. The scale of the map is 1 : 5,000,000 which was considered to be the largest possible for presenting a comprehensive picture of the world's soil resources based on the available data. This means that 1 cm on the map represents 50 km in the field (one inch represents about 80 miles). Therefore, this map gives regional information at scales > 250,000 but can never be used for the determination of soil properties at a specific location in the landscape.

The FAO Soil Map of the World recognizes 106 different soil units that were selected on the basis of available knowledge of the formation, characteristics and distribution of the soils covering the earth's surface, their importance as resources for production and their significance as factors of the environment. The soil units form the basis for about 5,000 different map units that consist of soil units or associations of soil units occurring within the limits of a mappable physiographic entity. When a map unit is not homogeneous –that is, when it does not consist of just one soil unit– it is composed of a dominant soil and associated soils. The latter cover at least 20 percent of the area; important soils that cover less than 20 percent of the area are added as inclusions. The textural class of the dominant soil and the slope class are given for each association. Phases are used where indurated layers or hard rock occur at shallow depth or in order to indicate stoniness, salinity and alkalinity. Climatic variants need to be considered for interpretation purposes.

In order to convert the qualitative soil information contained in the 106 FAO soil units to quantitative information, the International Soil Reference and Information Center (ISRIC) at Wageningen, The Netherlands, has compiled a high quality data base named the World Inventory of Soil Emission Potentials (WISE) that today contains more than 4382 soil profiles with quantitative soil information. ISRIC has linked the quantitative information in WISE with the qualitative global soil information in the FAO soil map using advanced taxotransfer rules[17]. This project has resulted in 28 quantitative physical and chemical soil properties that are needed for assessment of land suitability, crop growth simulation datasets, and analyses of global environmental change. ISRIC recommends the use of these quantitative parameters for regional to global studies on scales from 1:5,000,000 to 1:250,000. The physical properties for the top (0-30 cm) and subsoil (30-100) that are used in this study are: percentage of clay, sand, and silt; dry soil bulk density; and organic carbon content. Multiplication of the organic carbon content by two yields an estimate of the organic matter content in the soil.

### 3.2 Pedotransfer Functions for Soil Thermal Properties

The application of taxotransfer rules on the digitized FAO Soil Map of the World using the WISE data base of ISRIC results in maps of bulk densities, percentages sand, clay, and organic matter for the top and

subsoil for any region of interest. The next step is to convert these maps into maps of soil thermal properties using *pedotransfer functions*. A pedotransfer function is a mathematical relationship between two or more soil parameters that shows a high level of statistical confidence. In most cases it is used to estimate a non-measured soil parameter from one or more measured ones. In this study soil thermal properties are estimated from the bulk densities and percentages sand, clay, and organic matter for five different field soil moisture conditions.

The *volumetric heat capacity* of soil $C$ (MJ m$^{-3}$K$^{-1}$) is often expressed as the weighted sum of the heat capacities of the various soil constituents[18]. Since the volumetric heat capacity of air is about three orders of magnitude less than that of the other soil constituents it can be neglected so that the pedotransfer function becomes

$$C = \rho_b(c_m\psi_m + c_o\psi_o + c_w\theta_g) = \rho_b c_m\psi_m + \rho_b c_o\psi_o + c_w\theta_v = C_{solids} + c_w\theta_v \qquad [7]$$

where $c_s$, $c_o$, and $c_w$ are the specific heat of soil (0.73 kJ kg$^{-1}$K$^{-1}$), organic matter (1.9 kJ kg$^{-1}$K$^{-1}$), and water (4.18 kJ kg$^{-1}$K$^{-1}$), $C_{solids}$ is the volumetric heat capacity of the soil solids (minerals and organic matter), $\rho_b$ is the dry bulk density, $\psi_m$ is the mass fraction of soil minerals, $\psi_o$ is the mass fraction of organic matter content, $\theta_g$ is the gravimetric soil water content (kg kg$^{-1}$), and $\theta_v$ is the volumetric soil water content (m$^3$ m$^{-3}$).

*Soil thermal conductivity* ($\lambda$) can be determined from an empirical pedotransfer function[19].

$$\lambda = A + B\theta_v - (A - D)\, e^{-(C\theta_v)^4} \qquad [8]$$

where $\theta_v$ is the volumetric soil water content and $A, B, C, D,$ and $E$ are soil dependent coefficients which are related to soil properties that are usually fairly readily available. The relationships are

$$A = \frac{0.57 + 1.73\varphi_q + 0.93\varphi_m}{1 - 0.74\varphi_q - 0.49\varphi_m} - 2.8\phi_s(1 - \varphi_s)$$

$$B = 2.8\varphi_s$$

$$C = 1 + \frac{2.6}{\sqrt{\psi_m^{clay}}} \qquad [9]$$

$$D = 0.03 + 0.7\varphi_s^2$$

where $\varphi$ is the volume fraction of a particular component, subscripts "q", "m", and "s" indicate quartz, minerals other than quartz, and total solids, and $\psi_m^{clay}$ is the clay mass fraction. The thermal conductivity predicted by this equation is the total conductivity that includes the sensible and the latent heat components.

For the implementation of these thermal pedotransfer functions the mass and volume fractions of sand ($\psi_m^{sand}$ and $\varphi_m^{sand}$), silt ($\psi_m^{silt}$ and $\varphi_m^{silt}$), clay ($\psi_m^{clay}$ and $\varphi_m^{clay}$), and organic matter ($\psi_m^{om}$ and $\varphi_m^{om}$) are needed. The mass and volume fractions of the entire soil, including the soil minerals sand, silt and clay as well as organic matter are obtained from the weight percentages of sand (SA%), silt (SI%), clay (CL%), and organic matter (OM%) and the dry bulk density of the soil ($\rho_b$). The weight percentages of sand, silt, and clay total 100 percent while the weight percentage of organic matter is a percentage of the weight of the sum of sand, silt, and clay.

$$\psi_m^{sand} = \frac{SA\%}{SA\% + SI\% + CL\% + OM\%} \qquad \varphi_m^{sand} = \frac{\rho_b \times \psi_m^{sand}}{2650} \qquad \textbf{[10]}$$

$$\psi_m^{silt} = \frac{SI\%}{SA\% + SI\% + CL\% + OM\%} \qquad \varphi_m^{silt} = \frac{\rho_b \times \psi_m^{silt}}{2650} \qquad \textbf{[11]}$$

$$\psi_m^{clay} = \frac{CL\%}{SA\% + SI\% + CL\% + OM\%} \qquad \varphi_m^{clay} = \frac{\rho_b \times \psi_m^{clay}}{2650} \qquad \textbf{[12]}$$

$$\psi_m^{om} = \frac{OM\%}{SA\% + SI\% + CL\% + OM\%} \qquad \varphi_m^{om} = \frac{\rho_b \times \psi_m^{om}}{1500} \qquad \textbf{[13]}$$

When $\varphi_q$ is equal to zero, $\varphi_m = \varphi_m^{sand} + \varphi_m^{silt} + \varphi_m^{clay}$ and $\varphi_s = \varphi_m^{sand} + \varphi_m^{silt} + \varphi_m^{clay} + \varphi_m^{om}$. When the volume fraction of quartz is not zero, the thermal conductivity will increase considerably since the thermal conductivity of quartz minerals is approximately three times larger than that of the other soil minerals and about 44 times larger than that of organic matter. Unfortunately, the WISE data base has no information on the quartz content of the soils. In order to evaluate the possible effect of quartz on the thermal conductivity, one set of thermal properties will be evaluated assuming that the entire sand fraction consists of quartz ($\varphi_q = \varphi_m^{sand}$, $\varphi_m = \varphi_m^{silt} + \varphi_m^{clay}$ and $\varphi_s = \varphi_m^{sand} + \varphi_m^{silt} + \varphi_m^{clay} + \varphi_m^{om}$). This is not unreasonable since many sands worldwide contain a large portion of quartz minerals. However, there are also sands that contain no quartz at all.

After derivation of the volumetric heat capacity C and the thermal conductivity $\lambda$ the thermal diffusivity $\alpha$ (m$^2$ s$^{-1}$) is derived as

$$\alpha = \frac{\lambda}{C} \qquad\qquad\qquad \textbf{[14]}$$

### 3.3 Determination of Representative Field Soil Water Contents
Soil water contents in field soils depend on variable weather conditions and static soil hydraulic properties. There is no direct relation between environmental conditions and soil water content but a relationship exists between environmental conditions and soil water tension[2]. Considering the literature on volumetric water content at field capacity and the wilting point[1, 20, 21], we assume that in wet field soils the soil water pressure is about –70 cm, in moist field soils –330 cm, and in dried out field soils –15,000 cm. As extreme field moisture conditions "bone dry (i.e. water content zero)" and "saturated" are added. This results in five field soil moisture conditions: no water, dried out, moist, wet, and saturated. For the approximation of the soil water content at soil water pressures –70, -330, and –15,000 cm the linear regression equations [22] are used (Table 1).

### 3.4 Mapping Soil Thermal Properties
Combining the FAO-UNESCO Soil Map of the World with the WISE data base for different field soil water contents and different quartz contents in the sand fraction, one can map for any region of interest the thermal soil properties for the top (0-30 cm) and subsoil (30-100 cm). For example, in Figure 1 the map of thermal diffusivities is presented for a large area in Iraq and Iran.

---

[2]  In  unsaturated soils the soil water pressure is negative. Then, the soil water pressure is named the soil water tension.

Table 1. Linear Regression Equations for Predicting Soil Water Content at Specific Suctions from soil texture (sand and clay percentage), organic matter percentage and bulk density[22].

| Field Condition | Soil Water Pressure | Soil Water Pressure | Intercept a | Sand b | Clay c | Org. Matter d | Bulk Density E |
|---|---|---|---|---|---|---|---|
| | Cm | KPa | | % | % | % | g/cm³ |
| Wet | -70 | -7 | 0.7135 | -0.0030 | 0.0017 | | -0.1693 |
| Moist | -330 | -33 | 0.2576 | -0.0020 | 0.0036 | 0.0299 | |
| Dry | -15,000 | -1,500 | 0.0260 | | 0.0050 | 0.0158 | |
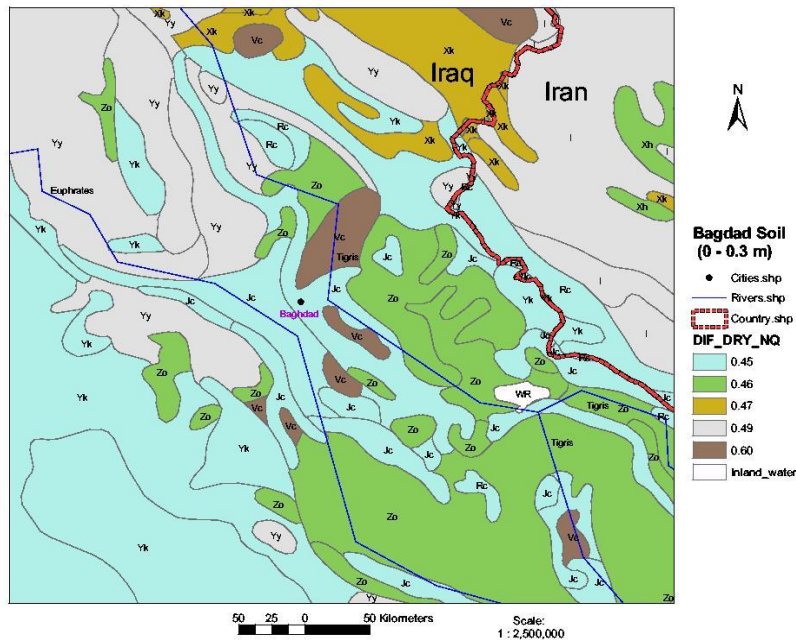


Figure 1. Soil thermal diffusivities for "dried out" soils around Baghdad, Iraq.

## 4. GLOBAL DISTRIBUTION OF THERMAL TOP AND BOTTOM SOIL BOUNDARIES

In Section 2 it has been shown that soil thermal regimes are not only determined by the thermal soil properties but also by the thermal boundary conditions. The thermal bottom soil boundary is the average annual soil profile temperature $T_{avg}^{annual}$ (°C); it is a general bottom boundary frequently used for the derivation of analytical solutions of the soil heat flow Eq. [1] as well as for numerical solutions such as implemented in HYDRUS1D. Frequently used thermal top boundary conditions for analytical solutions are the amplitude of the annual soil surface temperature variation $A_0^{annual}$ (°C) and the amplitude of the daily soil surface temperature variation $A_0^{daily}$ (°C). Numerical solutions can either use these harmonic functions of soil surface temperature or solve the complete energy balance at the soil surface[23].

### 4.1 Average Annual Soil Profile Temperature
Since the geothermal soil heat flux that transports heat from the center of the earth to its surface is very small compared to the daily and annual heat fluxes entering and leaving the soil body through the soil surface, it is reasonable to assume that the average annual soil profile temperature is approximately equal to

the average annual air temperature. In soil science the average annual soil temperature is often estimated [13] as

$$T_{avg}^{annual\_soil} = T_{avg}^{annual\_air} + 1 \qquad\qquad [15]$$

However, measurements at 21 sites covering the USA show that the differences between annual average soil temperature and annual average air temperature can fluctuate from -1.5 to 2.9 °C [24]. Yet, our own regression analysis of these data indicates that Eq. [15] is the best predictor of average annual soil temperatures for the 21 sites. In the former Soviet States measurements indicate differences ranging between 0.1 to more than 5 °C [24].

Soil temperature data presented by Van Wijk (1963) and average annual air temperatures per country found on the internet (www.tyndall.ac.uk) also corroborate Eq. [15] (Table 2). Including these data in our regression analysis of the USA data, Eq. [15] remains the best predictor of average annual soil temperature from average annual air temperature. The robustness of Eq. [15] is rather fortunate since there is no alternative method for the prediction of the average annual soil temperature except for measuring it. This can be accomplished by either one single measurement of soil temperature at great depth (10-20 m) or by calculating the average temperature of continuous measurements of soil temperatures at shallower depths for at least one year.

Table 2. Comparison of mean annual soil profile temperature (MAST) and mean annual air temperature (MAAS). Based on soil temperature data from Van Wijk (1963) and mean annual air temperature data per country found on www.tyndall.ac.uk.

| Country | MAST °C | MAAT °C | Difference °C |
|---|---|---|---|
| Finland | 2 | 1 | 1 |
| Germany | 9 | 9 | 0 |
| Indonesia | 29 | 27 | 2 |
| Japan | 16 | 15 | 1 |
| The Netherlands | 10 | 10 | 0 |

**4.2 Amplitude of Annual and Daily Soil Surface Temperature**
The variation of the soil surface temperature is mainly determined by the changing intensity of the short-wave radiation during the day and during the year as is demonstrated by soil temperature measurements at shallow depths worldwide[3]. Both the annual and daily amplitude of soil surface temperature are affected by the vegetative cover of the soil: bare soils will have larger amplitudes than vegetated soils[3, 25]. Therefore, the prediction of annual and daily soil surface temperature amplitudes for all soil surface conditions is not an easy task.

In hydrology remote sensing it has been observed that the surface temperature of moist pixels is approximately equal to the air temperature[26-29] since most available energy is used for evapotranspiration instead of for heating the soil surface. Recognizing that most meteorological stations are covered by a relatively well-watered short grass, we expect the annual soil surface temperature amplitude at these stations to approximate the annual near-surface air temperature amplitude. This hypothesis is tested in Table 3 using data obtained at different latitudes. Although the annual soil surface temperature amplitude varies from 1 C° to 23 C°, the difference between the amplitudes of soil and air temperatures varies from -3 to 2 C°. This suggests that for global applications a first minimum estimate of the annual soil surface temperature amplitude can be obtained from the annual air surface temperature amplitude. The same argument can also be made for the daily soil surface temperature amplitude: if all available energy is used for evapotranspiration the soil surface will have approximately the same temperature as the air.

Table 3. Comparison of amplitude of annual soil profile temperature and amplitude of annual air temperature. Based on soil temperature data from Van Wijk (1963) and air temperature data per country on www.tyndall.ac.uk.

| Location | Latitude | Longitude | Amplitude Soil °C | Amplitude Air °C | Difference °C |
|----------|----------|-----------|-------------------|------------------|---------------|
| Djakarta | 6S | 107E | 1 | 1 | 0 |
| Ikengueng | 42N | 108E | 18 | 20 | -2 |
| Potsdam | 52N | 13E | 11 | 14 | -3 |
| Sodankyla | 67N | 27E | 23 | 21 | 2 |

If it is necessary to evaluate soil thermal regimes for a wide range of environmental conditions on a daily and/or annual basis the best approach is to use a numerical model. For example, the HYDRUS1D code solves the coupled equations governing liquid water, water vapor, and heat transport, together with the surface water and energy balance, and provides flexibility in accommodating various types of meteorological information to solve the surface energy balance[14, 23]. Input information required for HYDRUS1D is soil textural information from the WISE data base, soil thermal properties derived from the pedotransfer functions (section 3.2), the average annual soil temperature (section 4.1), and meteorological data for the region of interest

The HYDRUS codes[14, 30] have been used by our research team for the simulation of soil moisture and dielectric regimes around landmines[31, 32] as well as for the simulation of thermal soil regimes around landmines[9]. HYDRUS1D has been used for the evaluation of the effects of wind speed on thermal landmine signatures[5].

## 5. SUMMARY AND FUTURE WORK

In this contribution we have described a procedure for the evaluation of global thermal soil regimes. First, pedotransfer functions are used to derive thermal soil properties (volumetric soil heat capacity and thermal conductivity) from readily available soil data on texture, bulk density, and organic carbon for different field soil moisture conditions. Next, the average annual soil temperature –i.e. the thermal bottom boundary needed to solve the heat flow equation by analytical or numerical means– is derived from the average annual air temperature using Eq. [15]. Then, the thermal top boundaries are derived either for well-watered sites using the daily and annual air temperature amplitudes as proxies for the daily and annual soil surface temperature amplitudes or for a wide range of environmental conditions using the model HYDRUS1D.

Our current implementation is a static one that doesn't account for real time soil moisture conditions. Work is underway to merge nearly real-time root zone soil moisture maps derived from Landsat and MODIS images[33, 34] into the developed procedure for nearly real-time mapping of thermal soil regimes for any region of interest worldwide.

The fraction of quartz minerals in the sand fraction of a soil influences the thermal conductivity. Therefore, we need to develop an approach to estimate quartz mineral content in soils using geological and soil data bases.

A thorough validation of the proposed procedure is needed for the quantification of the probability with which soil thermal regimes can be predicted. Of special interest is to quantify the relationship between the accuracy with which different soil properties (texture, bulk density, water content) are estimated and the quality of the predicted thermal soil regime.

## 6. ACKNOWLEDGEMENT

## 7. REFERENCES

1. Hillel, D., *Environmental soil physics*. 1998, San Diego, CA: Academic Press. 771.
2. Jury, W.A. and R.E. Horton, *Soil physics. Sixth Edition*. 2004: John Wiley & Sons, Inc. 370.
3. Van Wijk, W.R., *Physics of plant environment*. 1963: John Wiley & Sons, New York. 382.
4. Jacobs, P.A., *Thermal infrared characterization of ground targets and background. Second Edition.* Tutorial Texts in Optical Engineering. Vol. Volume TT70. 2006, Bellingham, WA: SPIE Press. 184.
5. Kleissl, J., et al., *HYDRUS simulations of soil surface temperatures.* Proc. International Society for Optical Engineering, SPIE, 2007. **6553**: p. 65530W 1-12.
6. Hendrickx, J.M.H., et al., *New Mexico Tech landmine, UXO, IED detection sensor test facility: measurements in real field soils.* Proc. International Society for Optical Engineering, SPIE, 2006. **6217**: p. 278-289.
7. Hong, S.-H., et al., *Impact of soil water content on landmine detection using radar and thermal infrared sensors.* Proc. International Society for Optical Engineering, SPIE, 2001. **4394**: p. 409-416.
8. Hong, S.-H., et al., *Land mine detection in bare soils using thermal infrared sensors.* Proc. International Society for Optical Engineering, SPIE, 2002. **4742**: p. 43-50.
9. Šimünek, J., J.M.H. Hendrickx, and B. Borchers, *Modeling transient temperature distributions around landmines in homogeneous bare soils.* Proc. International Society for Optical Engineering, SPIE, 2001. **4394**: p. 387-397.
10. Hendrickx, J.M.H., et al., *Scintillometer networks for calibration and validation of energy balance and soil moisture remote sensing algorithms.* Proc. International Society for Optical Engineering, SPIE, 2007. **6565**: p. 65650W.
11. Hendrickx, J.M.H., J. Kleissl, and S.-h. Hong, *Scintillometry for improved estimates of regional distributions of sensible and latent heat fluxes from MODIS images.* Annual Meeting Soil Science Society of America, 2006. **Abstract 41-3**: p. http://a-c-s.confex.com/crops/2006am/techprogram/P25864.HTM.
12. Kleissl, J., et al., *Large aperture scintillometer intercomparison study.* Boundary Layer Meteorol., 2008: p. in press.
13. Soil Survey Staff, *Soil Taxonomy. A basic system of soil classification for making and interpreting soil surveys. Second Edition.* 1999: United States Department of Agriculture - Natural Resources Conservation Service. 869.
14. Šimünek, J., M. Šejna, and M.T.V. Genuchten, *The HYDRUS-1D software package for simulating the one-dimensional movement of water, heat, and multiple solutes in variably saturated media. Version 2.0.* Vol. IGWMC-TPS-70. 1998, Golden, Colorado: International Ground Water Modelling Center, Colorado School of Mines. 202.
15. Elias, E.A., et al., *Anlytical soil-temperature model-correction for temporal variation of daily amplitude.* Soil Sci Soc Am J, 2004. **68**(3): p. 784-788.
16. FAO, *FAO Soil map of the world*, in *APDC/01/REP RAP PUBLICATION: 2001/14*. 1974, United Nations Educational, Scientific and Cultural Organization: Paris, France. p. pp. 59.
17. Batjes, N.H., *Soil parameter estimates for the soil types of the world for use in global and regional modeling. Versión 2.1.* Vol. ISRIC Report 2002/02c. 2002, Wageningen, The Netherlands: International Soil Reference and Information Center.
18. Kluitenberg, G.J., *Heat capacity and specific heat*, in *Methods of Soil Analysis. Part 4. Physical Methods*, J.H. Dane and G.C. Topp, Editors. 2002, Soil Science Society of America Book Series #5: Madison, Wisconsin. p. 1201-1208.
19. Bristow, K.L., *Thermal conductivity*, in *Methods of Soil Analysis. Part 4. Physical Methods*, J.H. Dane and G.C. Topp, Editors. 2002, Soil Science Society of America Book Series #5: Madison, Wisconsin. p. 1209-1226.
20. Cassel, D.K. and D.R. Nielsen, *Field capacity and available water capacity*, in *Methods of Soil Analysis, Part I. Agronomy Monograph Series No. 9. Second Edition.*, A. Klute, Editor. 1986: Madison, WI. p. 901-926.
21. Kirkham, M.B., *Principles of soil and plant water relations*. 2005, New York: Elsevier - Academic Press. 500.

22.     Rawls, W.J. and D.L. Brakensiek. *Prediction of soil water properties for hydrologic modeling. Watershed management in the Eighties, ASCE, pp. .* in *Watershed Management in the Eighties.* 1985. New York: ASCE.

23.     Saito, H., J. Simunek, and B.P. Mohanty, *Numerical analysis of coupled water, vapor, and heat transport in the vadose zone.* Vadose Zone J., 2006. **5**: p. 784-800.

24.     Mount, H.R. and R.F. Paetzold, *The temperature regime for selected soils in the United States. Soil Survey Investigation Report No. 48.* 2002, United States Department of Agriculture, Natural Resources Conservation Service, National Soil Survey Center Lincoln, Nebraska. p. 267.

25.     Gupta, S.C., W.E. Larson, and D.R. Linden, *Tillage and Surface Residue Effects on Soil Upper Boundary Temperatures.* Soil Sci Soc Am J, 1983. **47**(6): p. 1212-1218.

26.     Allen, R.G., M. Tasumi, and R. Trezza, *Satellite-based energy balance for mapping evapotranspiration with internalized calibration (METRIC) - Model.* Journal of Irrigation and Drainage Engineering, 2007. **133**: p. 380-394.

27.     Bastiaanssen, W.G.M., et al., *SEBAL model with remotely sensed data to improve water-resources management under actual field conditions.* J. Irrig. and Drain. Engrg., ASCE, 2005. **131**(1): p. 85-93.

28.     Compaoré, H., et al., *Evaporation mapping at two scales using optical imagery in the White Volta Basin, Upper East Ghana* Physics and Chemistry of the Earth, Parts A/B/C, 2007: p. In Press doi:10.1016/j.pce.2007.04.021.

29.     Hendrickx, J.M.H. and S.-h. Hong, *Mapping sensible and latent heat fluxes in arid areas using optical imagery.* Proc. International Society for Optical Engineering, SPIE, 2005. **5811**: p. 138-146.

30.     Šimůnek, J. and M. Šejna, *Software package for simulating the two- and three-dimensional movement of water, heat, and multiple solutes in variably-saturated media. User manual. Version 1.02.* 2007, Prague, Czech Republic: PC-Progress. 202.

31.     Das, B.S., J.M.H. Hendrickx, and B. Borchers, *Modeling transient water distributions around landmines in bare soils.* Soil Science, 2001. **166**(3): p. 163-173.

32.     Hendrickx, J.M.H., B.S. Das, and B. Borchers, *Modeling distributions of water and dielectric constants around land mines in homogeneous soils.* Proc. International Society for Optical Engineering, SPIE, 1999. **3710**(2): p. 728-738.

33.     Fleming, K., J.M.H. Hendrickx, and S.-h. Hong, *Regional mapping of root zone soil moisture using optical satellite imagery.* Proc. International Society for Optical Engineering, SPIE, 2005. **5811**: p. 159-170.

34.     Hendrickx, J.M.H., et al., *Mapping energy balance fluxes and root zone soil moisture in the White Volta Basin using optical imagery.* Proc. International Society for Optical Engineering, SPIE, 2006. **6239**: p. 238-249.